3rd CEAS Air&Space Conference
21st AIDAA Congress

Climate impact assessment of varying cruise flight altitudes applying the CATS simulation approach

Alexander Koch[a], Benjamin Lührs[a], Katrin Dahlmann[b], Florian Linke[a], Volker Grewe[b], Markus Litz[c], Martin Plohr[d], Björn Nagel[a], Volker Gollnick[a] and Ulrich Schumann[b]

German Aerospace Center (DLR)
[a] Air Transportation Systems, Blohmstraße 18, 21079 Hamburg, Germany
[b] Atmospheric Physics, Münchner Straße 20, 82234 Oberpfaffenhofen-Wessling, Germany
[d] Simulation and Software Technology, Linder Höhe, 51147 Köln, Germany
[d] Propulsion Technology, Linder Höhe, 51147 Köln, Germany

Keywords: *Climate compatible Air Transport System, Climate impact assessment, Operational measures, Varying cruise altitudes, Distributed Design Environment.*

Abstract

The present paper describes a comprehensive assessment and modelling approach that was developed in the DLR project Climate compatible Air Transport System (CATS) with the goal to analyze different options to reduce the climate impact of aviation.

The CATS simulation chain is applied to assess the climate impact reduction potential (via CO_2, contrail-cirrus, H_2O, NO_x, ozone, methane, primary mode ozone) for the world fleet of a representative long-range aircraft operated on a global route network in the year 2006.

The average temperature response (ATR) and the direct operating costs (DOC) are calculated for flights with varying cruise flight altitudes and speeds.

The obtained results are expressed as relative changes with respect to the minimum DOC trajectory and assessed as cost-benefit ratio (ATR vs. DOC). The results are highlighted for a single route and transferred to the global route network, showing a large potential to reduce the climate impact of aviation for small to moderate increments on costs.

1 Introduction

Aviation has an influence on global warming through the emission of gaseous compounds, aerosols, particle matter and induced cloudiness. Aviation was assessed to account in 2005 for a total radiative forcing of 43 mW/m^2 (median) excluding the impact from linear contrails and aviation induced cirrus clouds [1]. A new study reports model based estimates for the global climate impact from contrail induced cloudiness (CIC) of 31 mW/m^2 for the year 2002, including the impact from linear contrails, contrail-cirrus clouds and resulting changes in natural cirrus cloudiness [2]. This estimate highlights the relevance of induced cloudiness in any aviation climate impact study.

Without any further measures the projected air traffic growth of 4.8% Revenue Passenger Kilometres (RPK) per year till 2036 [3] will largely surpass the estimated annual fuel efficiency improvements of 1-2% [4]. The rise of annual emissions rates will hence further increase the climate impact from aviation.

The Advisory Council for Aeronautical Research in Europe (ACARE) states in this sense that a social and climate compatible air

transportation system is required for a sustainable development of commercial aviation. To achieve such a sustainable air transport system, mitigation strategies have to be developed based on comprehensive assessments of the different impacting factors and reduction potentials.

The atmospheric response to anthropogenic perturbance results from complex interrelated processes of very different nature, spatial and temporal scales. The global climate impact from air traffic varies not only with the amount and type of emitted species, but also with altitude, latitude of emission and the underlying atmospheric conditions.

The assessment of the aviation related climate impact still holds large uncertainties. However Grewe et al. (2007) [4] and Dahlmann et al. (2009) [6] showed that a comparative evaluation of new aircraft technologies or operational procedures is possible by minimizing the uncertainties in climate impact changes by adequate Monte-Carlo simulations.

The assessment of options to reduce the climate impact from aviation by new technologies and operations requires expert knowledge from different disciplines and adequate models that sufficiently incorporate the driving impact factors. Such a comprehensive simulation and analysis approach was developed within the DLR project *Climate compatible Air Transport System* (CATS) and presented for the first time by the authors in 2009 [7]. The present paper presents an enhanced version of the CATS-simulation chain and its application to evaluate operational measures to reduce the climate impact of air traffic. The analyzed measures are independent from individual weather situations; they are based on climatologic mean values derived from daily variations in weather situations. Different cruise flight altitudes and speeds are assessed for the world fleet of a representative long range twin-jet configuration operated on a global route network containing 1178 routes. The study discusses the potential to mitigate climate impact expressed as changes in global average temperature response (ATR) and direct operating costs (DOC).

2 Climate impact from aviation

The climate impact from air traffic results from induced cloudiness and concentration changes of the atmospheric constituents caused by the emission of carbon dioxides (CO_2), nitrogen oxides (NO_x), sulfur oxides (SO_x), water vapour (H_2O) and aerosols [8]. These atmospheric perturbations change the terrestrial radiation balance and cause a radiative forcing (RF) that drives the earth-atmosphere system to a new state of equilibrium through a resulting temperature change.

CO_2 is an effective greenhouse gas and one of the major contributors to the global warming (28 mW/m^2 until 2005) caused by air traffic. The impact of CO_2 is independent from the location of emission due its long atmospheric lifetime.

But also non-CO_2 effects have a large impact on the radiative forcing as displayed in Figure 1.

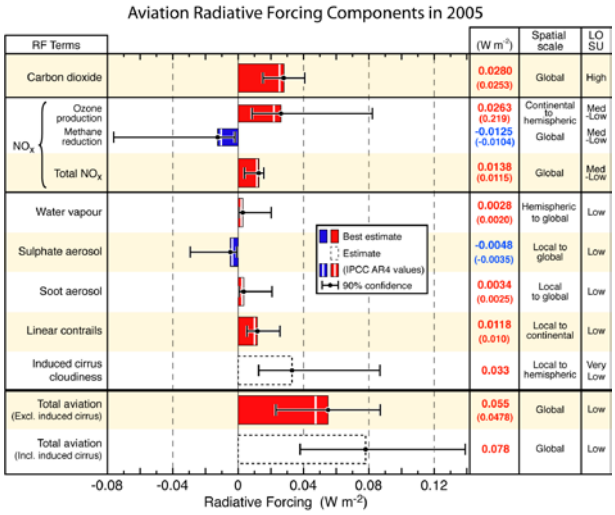

Fig. 1 Radiative forcings from global aviation as evaluated from preindustrial times until 2005 [1].

NO_x emissions from subsonic air traffic in the upper troposphere and lower stratosphere enhance the formation of ozone (O_3) and depletion of methane (CH_4), both compounds being greenhouse gases. The increased ozone concentration causes a warming effect (positive RF) whereas the reduction of atmospheric methane has a cooling effect (negative RF). Still, the net radiative forcing of NO_x is assumed to be positive (14 mW/m^2) as the impact of ozone prevails. The impact from NO_x emissions on the concentration change of ozone and

methane is sensitive to altitude and latitude. The maximum net radiative forcing is found at the tropical tropopause and decreases towards lower altitudes and higher latitudes [10]. This spatial dependency needs to be considered in the applied climate response model to correctly reflect the impact from aviation.

Volatile aerosols forming in young aircraft plumes are estimated to have a direct impact on the radiation budget through scattering and reflecting shortwave radiation (-5 mW/m^2) [12]. Aircraft-emitted soot particles are accounted to have a direct warming effect through absorption of shortwave and reemission of long-wave radiation (3 mW/m^2). Soot particles are key contrail-forming agents and are suspected to induce cirrus cloud formation. The latter effect is very uncertain because it is not known if these particles nucleate ice efficiently [12]. The estimated impact resulting from H_2O emitted at typical sub-sonic flight levels is comparatively small (3 mW/m^2) due to its small impact on the background concentration of H_2O.

Contrail induced cloudiness consists of linear contrails, contrail-cirrus clouds and of changes in the occurrence or properties of natural cirrus clouds. The formation and persistence of linear contrails depends on the atmospheric conditions, which have to be supersaturated with respect to ice and sufficiently cold [13][14]. This results in an altitude dependency [15]. Linear contrails transform to contrail-cirrus clouds under favourable meteorological conditions, able to cover large areas. For fixed ambient conditions, the impact of contrails depends mainly on the coverage and optical depth [16]. The global climate impact from CIC, including the impact from linear contrails, contrail-cirrus clouds and resulting changes in natural cirrus cloudiness, is modelled to account for 31 mW/m^2 [2]. CIC hence represents besides the impacts from NO_X and CO_2 a major contributor to climate change from air traffic.

Any climate response model applied to assess the impact from aircraft should consider the formation and impact of linear contrails and contrail cirrus by considering real weather situations [9] or climatologic averaged probabilities depending on altitude and latitude [10]. Further, any climate impact assessment not only requires the comprehensive modelling of non-CO_2 effects, but also a reasonable climate metric. Studies have shown that metrics like global warming potentials (GWP) or radiative forcing index (RFI) are easily misleading and not always appropriate for aviation studies [17]. Another approach to estimate the climate impact is the change of near-surface air temperature, as presented by Sausen and Schumann (2000) [18] or Grewe and Stenke (2008) [10]. The change of global average temperature response (ATR) [19] is a suitable metric for the purpose of the present study.

$$ATR_H = \frac{1}{H}\int_{t}^{t+H} \Delta T(t)dt \quad (1)$$

The presented metric integrates the surface temperature change $\Delta T(t)$ (expressed in °K) over a chosen time period H (for this study 100 years) considering thus impact of short-lived (e.g. contrails) and long-lived (e.g. CO_2) forcing agents in appropriate way.

3 Modelling the climate impact from aviation with the CATS approach

As outlined above, the climate impact from aviation depends among other factors within the earth-ocean-atmosphere system primarily on the emitted amount of the different species, the geographical position and altitude of emission as well as on the atmospheric background conditions.

The chemical and physical atmospheric processes that follow the emission of aircraft exhaust gases and lead to radiative forcing and temperature changes are partly interdependent and occur on very different spatial and temporal scales [3]. The identification and quantification of dependencies and driving factors within these highly complex processes requires large disciplinary expertise, simulation and experimental resources. Also the assessment of operational flight procedures, unconventional aircraft configurations and novel technologies asks for disciplinary expertise and proper model capabilities in the fields of air traffic management, flight performance and aircraft design with its related sub-disciplines

aerodynamics, structural design, systems, propulsion, etc. Altogether the required expert knowledge and model capabilities goes beyond the means of a single research engineer. Instead a group of experts and disciplinary models is required to reliably answer multidisciplinary research questions with such scale of complexity.

Within the DLR research project *Climate compatible Air Transport System* (CATS) such a comprehensive approach was developed to analyze the climate impact from air traffic, allowing the environmental and economical evaluation of new aircraft technologies, designs and operational procedures [7]. The CATS approach comprises models for appropriate physical simulation of aircraft design and performance, propulsion and emissions, mission calculation, climate response and operating costs. All models are developed and supervised by experts from the related fields. The setup of simulations and analysis of results is done in a collaborative way ensuring reliable conclusions.

3.1 Collaborative analysis capability

As argued above, the assessment of complex multidisciplinary topics requires a range of experts and models. Commonly the experts from research and/or industry entities are not located at the same location but regionally distributed.

This leads to the need of a distributed design and analysis environment that links the integrated disciplinary analysis models and provides means for the remote triggering, overall process control, convergence and optimization. The chosen model-based architecture and the underlying software engineering techniques influence the efficiency of the resulting analysis processes [20]. With increasing complexity of the model chain the number of interfaces is the critical factor for the flexibility of a design environment. Therefore a common namespace (central data model) is required for the efficient exchange of data and increased flexibility in model substitution [20].

Activities to establish such a collaborative analysis capabilities at DLR have started in 2005. Based on these activities, the central data model *Common Parametric Aircraft Configuration Scheme* (CPACS)[ii] and modelling environment *Remote Component Environment* (RCE)[viii] have been developed and applied in various projects. Both, RCE and CPACS will be made open source in 2011.

RCE [22] allows the linking of models provided by DLR entities and industry partners. The workflows can be started locally on the computer of the integrator or transferred to another platform. The models run on their server at the respective partner sites. CPACS [20][21] is based on XML technologies and includes the parametric description of the atmosphere, aircraft and engine performance, mission profiles, airports, fleet network as well as the resulting trajectories, climate impact and cost break down. Figure 2 shows the principle of collaborative design and analysis process as it is applied in CATS.

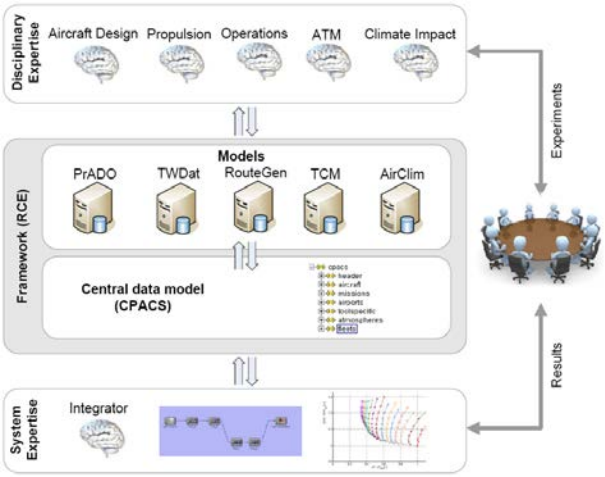

Fig. 2 DLR collaborative design and analysis process as applied in CATS.

3.2 CATS simulation chain

The integrated analysis models are provided by several DLR institutions and academia as listed at the end of this document (index *i-viii*). Plausibility of single model and overall simulation results are ensured by the involved experts in collaborative way. The outlined simulation process is displayed in Figure 3 and shows the simulation sequence of models.

The multi-disciplinary aircraft design tool *Preliminary Aircraft Design and*

Optimization[viii] (*PrADO*) developed by Technical University Braunschweig is applied to calculate the flight performance and technical characteristics of actual and novel aircraft configurations. *PrADO* comprises physical models with semi-empirical extensions for aerodynamics, structural analysis, weight prediction, flight performance incl. trim calculations and geometry description [22]. *PrADO* is further applied to determine the influence of aircraft subsystems on engine performance through bleed air and shaft power extraction.

The surrogate database model *TWdat*[iii] provides engine performance maps for several actual engines and possible future propulsion concepts, which are pre-calculated by the well-established thermodynamic cycle program *Varcycle*[iii] [24] and fitted to real engine data where possible. The performance maps contain emission indices (i.e. CO, NO_x, UHC, soot), thrust and fuel flow characteristics.

Models for preliminary flight preparation (*RouteGen*[ii] and *FuelEstimator*[ii]) provide relevant data concerning the mission profile (airports, lateral flight path, yearly frequencies) and estimation of required mission fuel and resulting payload limitations for all analyzed routes.

The *Trajectory Calculation Module* (*TCM*)[ii] is applied to calculate detailed emission inventories with 4D trajectories. *TCM* performs a fast-time simulation integrating the relevant flight conditions based on the total energy model [25]. It reads as input mission parameters, aircraft weight breakdown, engine and aerodynamic performance tables for different high-lift configurations provided by *PrADO* and *TWDat*. This capability enables the flight performance simulation and evaluation of novel aircraft concepts.

The model *FlightEnvelope*[ii] checks each calculated flight trajectory if aircraft specific operating constraints (stall, buffet and altitude limits) are violated. In such case the concerning trajectories are removed from the dataset.

Annual mean atmospheric data includes temperature, pressure, relative humidity, wind vectors as function of latitude and altitude are provided by the model *Atmos*[i].

The climate impact of each flight is assessed with the climate response model *AirClim*[i] [10][11]. The model comprises a linearization of a climate-chemistry model from the emission to radiative forcing, resulting in an estimate in near surface temperature change, which is presumed to be a reasonable indicator for climate change. AirClim is designed to be applicable to aircraft technology, considering the altitude and latitude of emission for the climate agents CO_2, H_2O, CH_4, O_3 and primary ozone mode (PMO) (latter three resulting from NO_x emissions), line-shaped contrails and contrails cirrus clouds. Combining aircraft emission data with a set of previous calculated atmospheric perturbations, AirClim calculates the radiative forcing and resulting temporal evolution of global near surface temperature change. The pre-calculated data are derived from 78 steady-state simulations for the year 2000 with the DLR climate-chemistry model *E39/CA*, prescribing normalized emissions of nitrogen oxides and water vapour at various atmospheric regions [26].

The economical impact is calculated as direct operating costs (DOC)[ii] of each flight including the costs for fuel, crew, maintenance, navigation and landing fees and financing [27].

Depending on the scope of study, different process control scripts are integrated for the variation of routes or aircraft configurations.

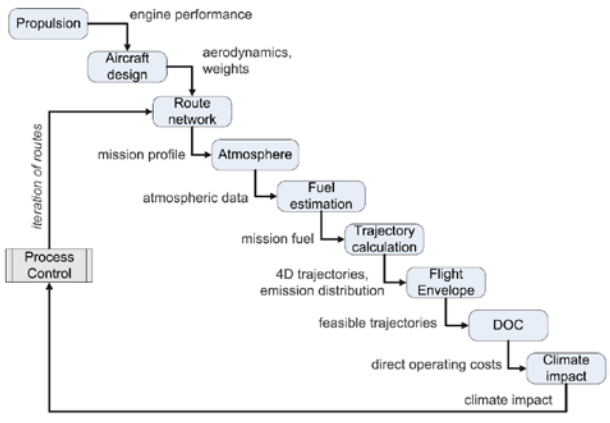

Fig. 3 Simulation sequence as applied in CATS.

4 Calculating the climate impact of varying cruise flight altitudes and speeds

The goal of the present study is to apply the CATS approach to identify the potential of climate impact reduction and related DOC changes through varying cruise flight altitudes and speeds based on the world fleet of a representative long range aircraft.

4.1 Setup of experiment

All routes operated in the year 2006 by an Airbus A330-200 are derived from OAG data [28] resulting in a set of 1178 global distributed city pair connections with corresponding flight frequencies.

The reference aircraft is modelled to fit the geometry, weights and performance characteristics of the real aircraft equipped with CF6-80E1A3 engines. Table 1 specifies the basic model characteristics and Figure 4 shows the resulting model geometry. Figure 5 displays the model payload-range performance in comparison to the real aircraft [29]. Note that the different slope in the payload range diagram comes from a slightly better SFC in the engine model. This leads to a 3.5% lower max take-off weight and an increased ferry range of 3.7%. Scaling of the model SFC is considered not appropriate because of the not fully quantifiable impact on emission indices, which are considered of higher priority to the study goal than a perfect fit of the reference aircraft.

Design conditions		
Design range	7861	km
Design cruise Mach	0.82	-
Design payload	253 PAX + 23.75 t	
Design ICA	10000	m
Resulting model characteristics		
Operational empty weight	116.2	t
Max take-off weight	221.5	t
FAR Take-off field length	2389	m
FAR Landing field length	1690	m
Approach speed	75.5	m/s
L/D @ design conditions	19.9	-
SFC @ design conditions	0.05876	kg/N/h

Table 1 Model performance characteristics

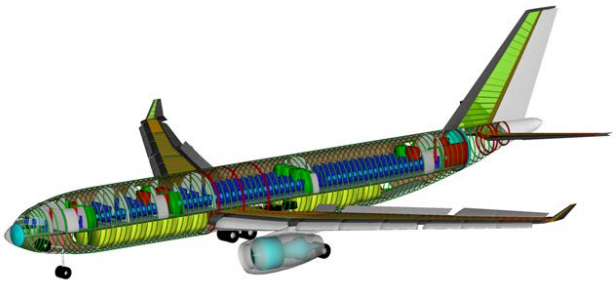

Fig. 4 Geometry model of reference aircraft.

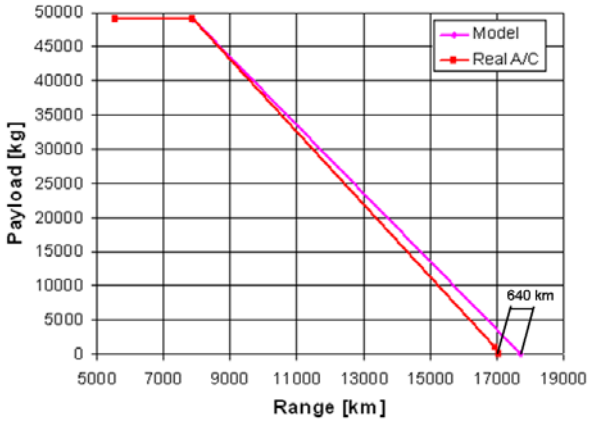

Fig. 5 Payload range comparison of model vs. real A/C

The vertical flight profile is based on typical flight phases and respects (where possible) the common air traffic control (ATC) speed and altitude constraints during climb and descend. The cruise phase is modelled as continuous climb cruise at constant lift coefficient. This is assumed an appropriate approximation to a real cruise flight with step climbs, which are normally optimized by flight planning tools for the specific route considering the actual transport conditions and ATC restrictions.

The operative payload is considered with an average passenger load factor of 0.76 and additional 5000 kg of cargo [3].

The DOC [$/cycle] are calculated without the cost of ownership (depreciation, interests, insurance) in order to assess the increment on flight operation costs only (cash operating costs). The average fuel price in 2006 (0.6 USD/kg) is derived from [30], cost values for labour (25 USD/h) and fees are based on [27] and scaled by the average US inflation rate (2.66%) from 1993-2006 [31].

The climate impact is calculated for sustained emissions over 32 years, which corresponds to the average lifetime of the reference aircraft [3]. The evolution of background emissions of CO_2 and CH_4 follow the IPCC scenario A1B [32] while the development of background air traffic for contrails-cirrus assessment is based on data from the *QUANTIFY* emission inventory [33] scaled by IPCC scenario Fa1 [8]. The average temperature response is evaluated for the time frame of H=100 years (ATR_{100}) starting in 2006.

For each route (index i), cruise Mach numbers from 0.4 to 0.85 in steps of 0.025 and initial cruise altitudes (ICA) from 3962-12497m (=13kft to 41kft) in steps of 305m (=1kft) are analyzed with the described settings. Each Ma_{cr}–ICA combination represents one cruise operating point. The authors would like to emphasize that the wide ranges of ICA and Ma_{cr} values are chosen to identify the maximum potential of climate impact reduction, reflecting less the actual ATC practice.

4.2 Evaluation methodology

For each cruise operating point and resulting trajectory (index *k*) the reduction potential is expressed as cost-benefit ratio (ATR_{rel} vs. DOC_{rel}) relative to the route-specific cruise operating point for minimum DOC (DOC_{min}).

There are still many uncertainties in the calculation of the climate impact of air traffic [1]. To account for these uncertainties a Monte-Carlo simulation is performed in such way that AirClim calculates a minimum and maximum temperature change for each species and each uncertainty specified in [10]. For each species 10000 random values α_j are picked within the given distribution of the uncertainty range for each uncertainty parameter (Radiative Forcing and climate sensitivity for each species, as well as stratospheric and tropospheric lifetimes). The respective climate impact for each species is calculated for each step j of the Monte Carlo simulation

(2) $ATR_{spec}(j) = \alpha_j \, ATR_{min}(j) + (1 - \alpha_j) ATR_{max}(j)$

Based on this, the relative difference (φ) between the trajectory *k* and reference trajectory for each step j of the Monte Carlo simulation can be determined.

$$(3) \qquad \varphi_k(j) = \frac{ATR^k_{spec}(j) - ATR^{ref}_{spec}(j)}{ATR^{ref}_{spec}(j)}$$

Where $ATR^k_{spec}(j)$ is the average temperature change resulting from the impact of a certain species on trajectory *k* and $ATR^{ref}_{spec}(j)$ is the temperature change for the reference trajectory, in this study the route-specific cruise operating point for minimum DOC (DOC_{min}). The total climate impact $ATR^k_{all}(j)$ for one trajectory and route is given by the sum of impacts from all species. For the different $\varphi_k(j)$ resulting from the Monte Carlo simulation, the median and the 2.5, 25, 75 and 97.5% percentiles are calculated and serve as uncertainty range. This specific Monte-Carlo calculation takes advantage of the lower uncertainty of the relative difference between the climate impacts of two scenarios compared to their individual absolute values [11].

The ATR_i and DOC_i changes relative to $DOC_{min,i}$ are calculated for all feasible operating points (Ma_{cr}, ICA) on route (*i*).

$$(4) \; DOC_{rel,i}(Ma_{cr}, ICA) = \frac{DOC_i(Ma_{cr}, ICA)}{DOC_{\min,i}}$$

$$(5) \; ATR_{rel,i}(Ma_{cr}, ICA) = \frac{ATR_i(Ma_{cr}, ICA)}{ATR_i(Ma_{cr}, ICA)_{DOC_{\min,i}}}$$

Plotting $DOC_{rel,i}$ vs. $ATR_{rel,i}$ for all calculated operating points in one diagram per route yields a Pareto front of best solutions that displays the climate impact reduction potential as function of the related increment in DOC relative to the route specific operating point for minimum DOC. As such relation is only given for computed Ma_{cr}–ICA combinations, the information about the corresponding operating point is lost for interpolations between Pareto elements. To determine hence the largest relative climate impact reduction for an accepted maximum cost increment *x* (e.g. *x*=1.10) on each route, the route-specific Pareto front is intersected at the defined *x* value and

evaluated for the next smaller available operating point on the curve. The resulting $DOC_{rel,i}(\tilde{x})$ and $ATR_{rel,i}(\tilde{x})$ values have thus to be considered as best solution $\tilde{x}$ that fulfils the specified cost limit x on a specific route.

The $DOC_{min,i}$ operating point and corresponding absolute ATR_i vary for each route depending on fuel burn, flight time and latitude of emission.

To estimate the reduction potential resulting from all routes ($ATR_{rel,all}(\tilde{x})$), every Pareto front is intersected at the specified maximum DOC increment x and evaluated at the next smaller Pareto Element $\tilde{x}$. The related $ATR_i(\tilde{x})$ values are weighted by the route specific flight frequency (f_i) and summed for all routes.

$$(6)\quad ATR_{rel,all}(\tilde{x}) = \frac{\sum_{i=1}^{n\_routes} f_i \cdot ATR_i(Ma_{cr}(\tilde{x}), ICA(\tilde{x}))}{\sum_{i=1}^{n\_routes} f_i \cdot ATR_i(Ma_{cr}, ICA)_{DOC\,min,i}}$$

The same approach is applied to determine the overall $DOC_{rel,all}(\tilde{x})$ and uncertainty range for $ATR_{rel,all}(\tilde{x})$, which is based on the percentiles of each specific route.

5 Discussion of results

To provide an overview about the study results and trends the route Detroit-Frankfurt (DTW-FRA) is discussed exemplarily. Figures 6 and 7 show DOC_{rel} and ATR_{rel} respectively for varying cruise Mach number with fixed ICA [a] and vice-versa [b]. The operating point for minimum DOC on route FRA-DTW was found at Ma=0.85 and ICA=10973m.

Figure 6a shows the evolution of DOC_{rel} with varying Ma_{cr} for constant ICA. For this case the total DOC_{rel} curve shows a variation of 43% over the plotted Ma range and follows largely the trend of the time dependent costs (crew, maintenance). The fuel costs are proportional to the fuel burn and show in this case a minimum for Ma_{cr}=0.675, rising to lower and higher speeds due to the increased drag and required thrust.

Figure 6b displays DOC_{rel} for fixed Ma_{cr} and varying ICA, which experiences a variation of 9% over the analyzed ICA range. The impact of ICA on the time dependent costs is in this case very small due to subtle changes in flight time. This leads to a total DOC evolution that follows the fuel costs curve, which has a minimum at ICA=10973m.

These two graphs indicate that the evolution of DOC is primarily driven by the cruise Mach number through its impact on maintenance and crew costs. Note that this trend (decreasing total DOC towards higher speeds) is influenced by the costs assumptions in the study scenario [27], which assumes a relative low fuel price compared to the labor costs.

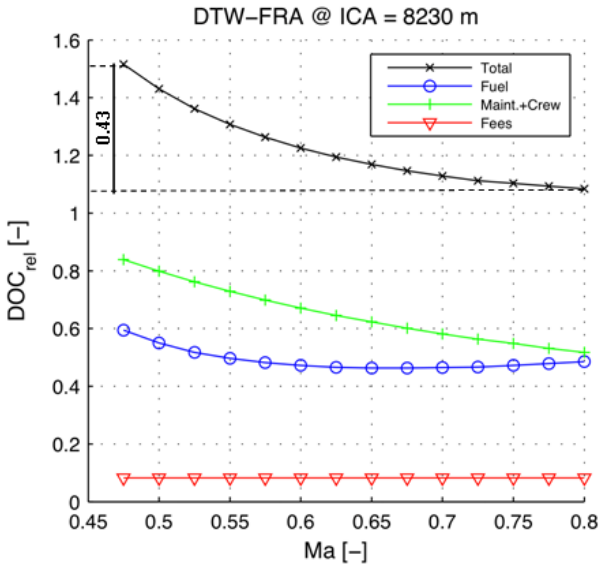

Fig. 6a Relative DOC changes for ICA=8230m and varying cruise Mach numbers on route DTW-FRA.

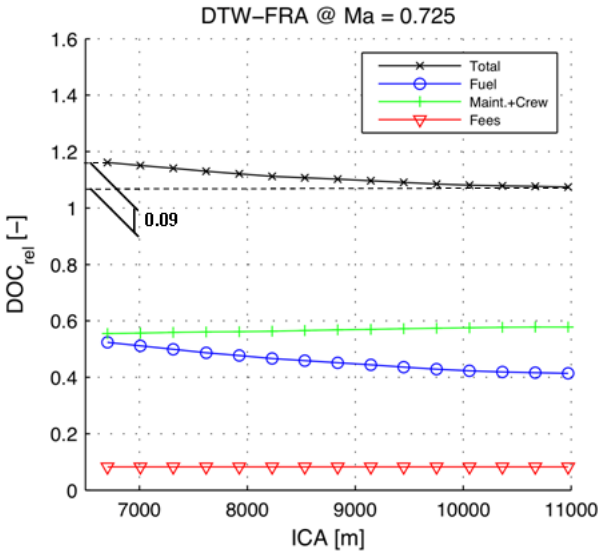

Fig. 6b Relative DOC changes for Ma=0.725 and varying ICA's on route DTW-FRA.

Figure 7a displays the evolution of ATR_{rel} with varying Ma_{cr} for constant ICA, showing a variation of 12% between the minimum at Ma=0.625 and maximum at Ma=0.475. In this case the amount and related impact of emitted CO_2 is proportional to the fuel burn (3.15 kg CO_2/kg fuel) and follows the trend displayed in Fig. 6a, whereas the impacts from O_3 and CH_4 are related to the emitted amount of NO_x (at constant altitude). At both ends of the fuel burn curve the NO_x emission index (kg NO_x/kg fuel) rises and provokes thus an increased impact from O_3 (warming) and from CH_4 (cooling). The formation and related impact from contrails and contrail-cirrus (index *cont*) is not sensitive to speed changes as the modeled formation of contrails is dependent on altitude. The impact resulting from PMO (primary mode ozone) is proportional to CH_4. The impact from H_20 is almost independent from Ma_{cr}, showing only a very small dependency from fuel burn at constant altitude.

Figure 7b shows ATR_{rel} for fixed Ma_{cr} and varying ICA, exhibiting a variation of 32% over the analyzed ICA range with increasing reduction potential for decreasing altitudes. Here the impact from O_3 dominates at higher altitudes, increasing steeply above approx. 9500m. This increase is largely caused by the rising sensitivity of O_3 production with higher altitudes, whereas the increase in emitted NO_x contributes also but is not the dominant effect. CH_4 displays a light dependency from altitude, its cooling impact diminishing slightly with increasing altitude. The same applies to PMO, being proportional to CH_4, only at smaller magnitude. The formation of contrails and contrail-cirrus has its maximum on this route at ICA=9449m, decreasing to lower and higher altitudes. The CO_2 impact decreases for higher altitudes as fuel burn decreases (compare Fig. 6b). The emitted amount of H_20 is proportional to fuel burn (1.25 kg H_20/kg fuel) and thus decreases with altitude, whereas the impact from H_20 instead increases due its increasing atmospheric lifetime. PMO shows a relative small dependency from altitude.

Figures 7a-7b highlight that the sole minimization of CO_2 (fuel burn) does not lead to the minimum climate impact. In fact, the minimization of CO_2 leads to higher altitudes while the minimum climate impact is obtained at lower altitudes (Fig. 7b).

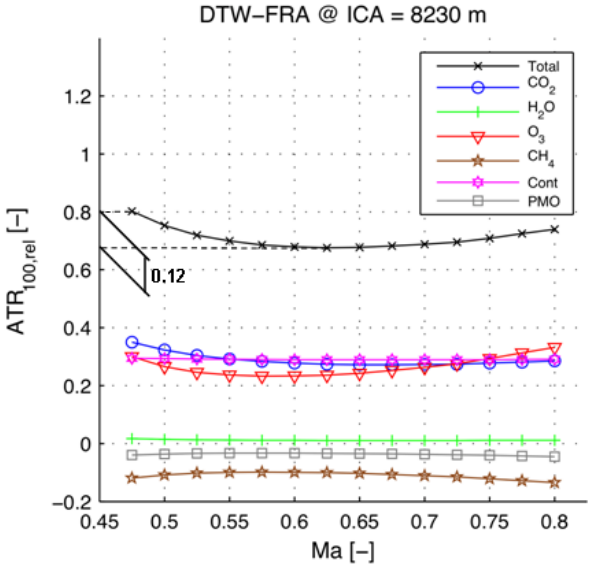

Fig. 7a Relative ATR changes for ICA=8230m and varying cruise Mach numbers on route DTW-FRA.

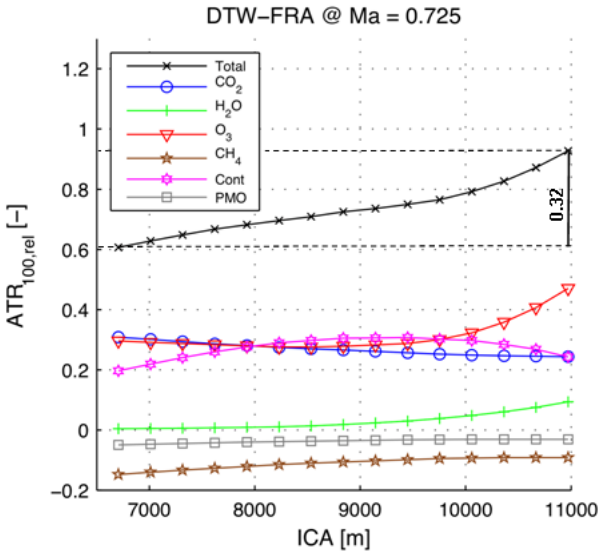

Fig. 7b Relative ATR changes for Ma=0.725 and varying ICA's on route DTW-FRA.

When comparing the relative importance of the different forcing agents it shows that impacts resulting from induced cloudiness, CO_2 and O_3 are having the largest contribution to the total climate impact. Among those, the impacts from O_3 and induced cloudiness show the largest variation due to ICA changes.

The reduction of cruise altitude therefore leads to a reduction in climate impact, even with

slightly increased fuel burn and related CO_2 impact. Resulting from the discussion of Figures 6a-6b the sensitivity of DOC with altitude changes is small in comparison to speed changes, which leads to the conclusion that a reduction of cruise altitude will have only a moderate impact on DOC.

This relation can also be observed in Figure 8 that shows the resulting ATR_{rel} and DOC_{rel} for all calculated operating points for the route DTW-FRA. The operating points are indexed for constant ICA values with increasing Mach numbers moving down the curves for constant ICA. The Pareto front contains all the Pareto optimal Ma_{cr} – ICA combinations between the reference point (DOC_{min}) and the operating point for maximum achievable ATR_{rel}.

Intersecting the DTW-FRA Pareto front exemplarily for a maximum DOC increment of 10% (x=1.1), the closest calculated operating point that fulfils this condition is found at ICA=8534 (light brown triangles) and Ma_{cr}=0.75. At this point a relative climate impact reduction of 28% (median), $ATR_{rel}(\tilde{x})$=0.72, is achieved with a corresponding DOC increment of 9.3%.

This ratio shows that a relatively large climate impact reduction is achievable for a comparably small cost increase.

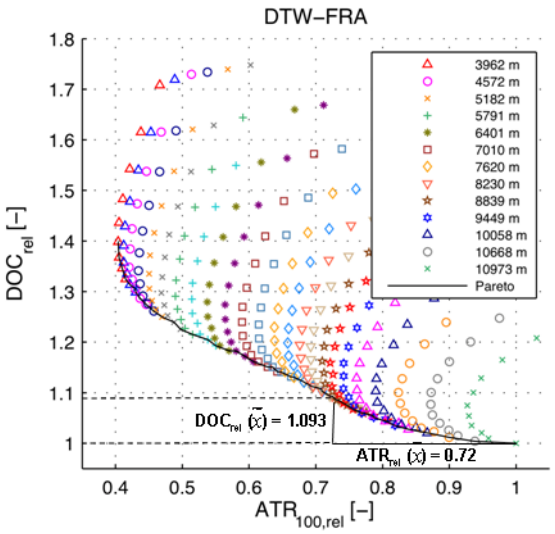

Fig. 8 Pareto front for route DTW-FRA obtained from all feasible operating points with resulting ATR_{rel} and DOC_{rel} values. Note that only every second ICA is displayed in the legend. ICA changes follow steps equivalent to 1000ft. Ma increases moving down the curves for constant ICA.

The DOC_{min} operating point and absolute ATR vary for each route, depending on the flight distance and feasible trajectories. Due to this, a different Pareto front and corresponding potential to reduce the climate impact is obtained for each route.

In order to identify the overall potential resulting from all routes operated by the reference aircraft in 2006, the approach described by Eq. 6 is applied. Figure 9 displays the $DOC_{rel,all}$ and $ATR_{rel,all}$ values based on all Pareto fronts. The error bars are calculated with Eq. 6 and indicate the percentile ranges for 25%-75% (blue) and 2.5%-97.5% (red), serving as measure of uncertainty for $ATR_{rel,all}(\tilde{x})$.

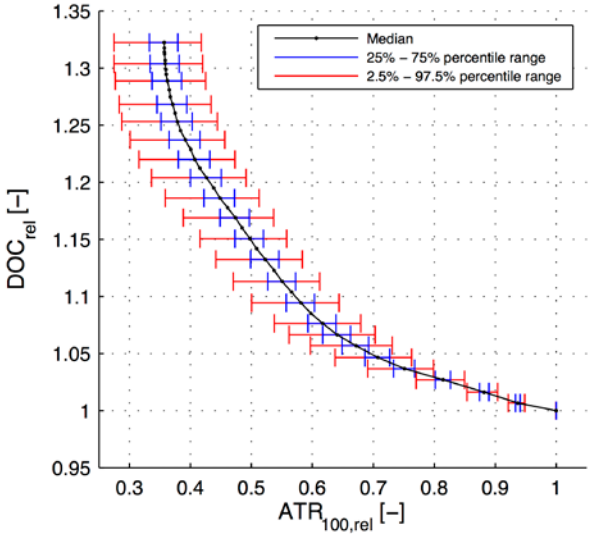

Fig. 9 $DOC_{rel,all}$ vs. $ATR_{rel,all}$ Pareto front for all routes operated with A330-200 in 2006. Error bars correspond to 25%-75% (blue) and 2.5%-97.5% (red) probability range.

The graph shows that the potential to reduce the climate impact by reduced cruise altitudes on all routes is still favourable, even better than on the route DTW-FRA. A maximum DOC increment of 9.5% relative to the DOC_{min} operating conditions on each route would yield a reduction of $ATR_{rel,all}$ between 36% and 50% (median 42%) when considering the 2,5%-97,5% percentile range.

The operating points corresponding to a given $DOC_{rel,all}(\tilde{x})$-$ATR_{rel,i}(\tilde{x})$ combination differ for each route, depending on the distance and payload. In order to infer from a given $DOC_{rel,all}(\tilde{x})$ back to the corresponding distribution of operating points, the Ma_{cr}-ICA

combinations at the route-specific $DOC_{rel,i}(\tilde{x})$ are plotted in a diagram Ma_{cr} vs. ICA for all route (Figures 10a-10b). The occurrence of operating points is expressed relative to the number of analyzed routes.

Figure 10a displays the distribution and relative occurrence of Ma_{cr}-ICA combinations with minimum DOC ($DOC_{rel,all}(\tilde{x})$=1) for all analyzed routes. As in Figures 6a-6b, the trend towards high Mach numbers and altitudes for DOC_{min} is clearly visible also in this graph. The majority of operating points are found at the highest possible Mach number 0.85 and ICA=12000m, while the rest is located in the near vicinity showing only a small variation.

Figure 10b shows the distribution of operating points for the exemplarily discussed $DOC_{rel,all}(\tilde{x})$=1.095. As described above, the decrease of ATR_{rel} and related increase of DOC_{rel} are connected to lower cruise altitudes and speeds. In the analyzed case the majority of operating points are located between 0.75≤Ma≤0.775 and 8000m≤ICA≤8500, showing a larger variation than for DOC_{min}.

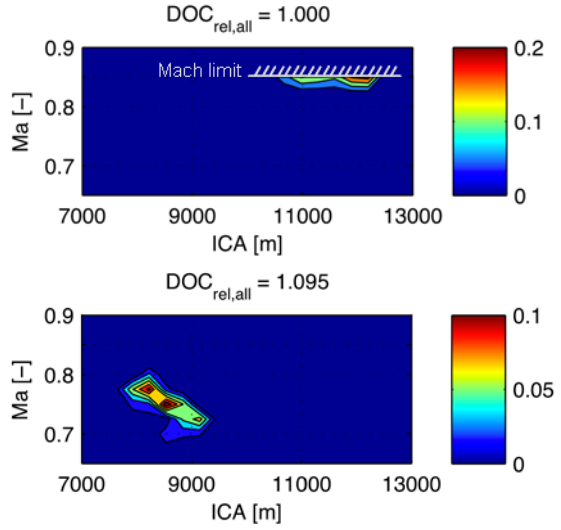

Fig. 10a-b Distribution and relative occurrence of all operating points for $DOC_{rel,all}$=1.00 (DOCmin) [a] and for $DOC_{rel,all}$=1.095 [b]

6 Conclusions

The present paper describes a comprehensive simulation and analysis approach developed at DLR to analyze different options to reduce the climate impact from aviation. The CATS simulation chain is applied to identify the potential to mitigate climate impact through reduced cruise flight altitudes on a global route network operated by a representative twin jet long-range aircraft in the year 2006. The study results are analyzed relative to the cruise operating conditions for minimum direct operating costs. The different impacts and trends on direct operating costs and average temperature response are discussed on the basis of a single route and transferred to the global route network. The distribution of relative occurrence of operating points for a given DOC increment is shown.

The present study found that the climate impact is mainly driven by altitude changes while the DOC are driven instead by speed changes. The study results further showed that there exists a large potential to reduce the climate impact from aviation for relative small to moderate increments on costs when the fleet of reference aircraft would be operated at lower cruise flight altitudes and speeds on all routes.

Future studies will focus on the potential that can be achieved when re-designing the reference aircraft for operating points with lower climate impact. Therefore a new design point will be derived from actual data. The reduction potential of the new aircraft will be discussed in comparison to the reference aircraft.

Acknowledgments

The following partner institutions contribute to the project *Climate compatible Air Transport System* (CATS) with expertise and models.

i. DLR - Atmospheric Physics
ii. DLR - Air Transportation Systems
iii. DLR - Propulsion Technology
iv. DLR - Combustion Technology
v. DLR - Flight Guidance
vi. DLR - Aerospace Medicine
vii. DLR - Simulation and Software Technology
viii Technical University Braunschweig - Aircraft Design and Lightweight Structures

Authors contact

Alexander Koch
German Aerospace Center (DLR)
Air Transportation Systems
Blohmstrasse 18
21079 Hamburg
Alexander.Koch@dlr.de
+49-40-42878-3634

References

[1] Lee, D.S., et al., *Aviation and global climate change in the 21st century*, Atmospheric Environment, 2009.

[2] Burkhardt, U., and Kärcher, B., *Global radiative forcing from contrail cirrus*, Nature Climate Change 1 (2011), 54–58, 2011.

[3] International Civil Aviation Organization – Committee on Aviation Environmental Protection, *FESG CAEP/8 Traffic and Fleet Forecasts*, CAEP-SG/20082-IP/02, 2008.

[4] Intergovernmental Panel on Climate Change, *Climate Change 2007 - Synthesis Report*, Cambridge University Press, 2007.

[5] Grewe, V., et al., *Climate impact of supersonic air traffic: an approach to optimize a potential future supersonic fleet – results from the EU project SCENIC*, Atmos. Chem. Phys., 7, 5129 5145, 2007.

[6] Dahlmann, K., at al., *Climate impact evaluation as part of aircraft pre-design*, 9th AIAA Aviation Technology, Integration, and Operations (ATIO) Conference, AIAA 2009-6957, 2009.

[7] Koch, A, et al., *Integrated analysis and design environment for a climate compatible air transport system*, 9th AIAA Aviation Technology, Integration, and Operations (ATIO) Conference, AIAA 2009-7050, 2009.

[8] Penner JE, Lister DH, Griggs DJ, Dokken DJ, McFarland M., *Aviation and the Global Atmosphere*, Cambridge University Press, 1999.

[9] Schumann, U., Graf, K., Mannstein, H., *Potential to reduce the climate impact of aviation by flight level changes*, 3rd AIAA Atmospheric Space Environments Conference, AIAA 2011-3376, 2011.

[10] Grewe, V., Stenke, A., *AirClim: an efficient climate impact assessment tool*, Atmospheric Chemistry and Physics, 8, 4621- 4639, 2008.

[11] Dahlmann, K., Bewertung neuer Flugzeugtechnologien hinsichtlich ihrer Klimawirkung, PhDthesis, Ludwig-Maximilians-Universität München, to be published.

[12] Kärcher, B., Möhler, O, DeMott, P.J., Pechtl, S., Yu, F. *Insights into the role of soot aerosols in cirrus cloud formation*. Atmos. Chem. Phys. 7 4203-4227, 2007.

[13] Appleman, H. *The formation of exhaust contrails by jet aircraft*, Bull. Am. Meteorol. Soc. 34, 14-20, 1953.

[14] Schumann, U., *On conditions for contrail formation from aircraft exhausts*, Meteorol. Z., 5, 4 –23, 1996.

[15] Fichter, C., Marquart, S., Sausen, R., Lee, D.S., *The impact of cruise altitude on contrails and related radiative forcing*, Meteorologische Zeitschrift, 14, S. 563 – 572, 2009a.

[16] Meerkötter, R. et al. *Radiative forcing by contrails*, Ann. Geophys. 17, 1080-1094, 1999.

[17] Wuebbles, D.J., Yang, H., Herman, R., Climate *Metrics and Aviation: Analysis of Current Understanding and Uncertainties*, Aviation-Climate Change Research Initiative, 2008

[18] Sausen, R., Schumann, U., *Estimates of the climate response to CO2 and NOx emission scenarios*, Climatic Change 44, 27–58, 2000.

[19] Schwartz, E., Kroo, I. M., *Metric for Comparing Lifetime Average Climate Impact of Aircraft*, AIAA Journal, Vol. 49-8, 2011.

[20] Böhnke, D., Nagel, B., Gollnick, V., *An Approach to Multi-Fidelity in Conceptual Aircraft Design in Distributed Design Environments*, IEEE Aerospace Conf., 2011.

[21] Liersch, C., Hepperle, M., *A Unified Approach for Multidisciplinary Aircraft Design*, CEAS European Air and Space Conference, 2009.

[22] Bachmann, A., Kunde, M., Litz, M., Schreiber, A., *Advances in Generalization and Decoupling of Software Parts in a Scientific Simulation Workflow System*, 4th International Conference on Advanced Engineering Computing and Applications in Sciences (ADVCOMP) , 2010.

[23] Heinze, W., Ein Beitrag zur quantitativen *Analyse der technischen und wirtschaftlichen Auslegungsgrenzen verschiedener Flugzeugkonzepte für den Transport großer Nutzlasten*, PhD-thesis TU Braunschweig, ZLR Forschungsbericht 94-01, 1994.

[24] Deidewig, F., *Ermittlung der Schadstoffemissionen im Unter- und Überschallflug*, PhD-thesis, 1998.

[25] Linke, F., *Trajectory Calculation Module*, DLR internal report, LK-IB 001-2008, 2008.

[26] Fichter, C., *Climate impact of air traffic emissions in dependency of the emission location and altitude*, Manchester Metropolitan University, 2009b.

[27] Liebeck, R. H., et al., *Advances in subsonic airplane design & economic studies*, NASA CR 195443, 1995.

[28] OAG Aviation Solutions, *Airline schedule and aircraft fleet databases*, 2006.

[29] Airbus S.A.S., *A330 Airplane Characteristics for Airport Planning*, 1993.

[30] ESG Aviation Services, *The Airline Monitor, Vol. 20 No. 6*, Edmund S. Greenslet, 2007.

[31] International Monetary Fund, *World Economic Outlook Database*, Sept. 2006, accessed 2011.

[32] Nakicenovic, N., et al., *Special Report on Emissions Scenarios: A special report of Working Group III of the Intergovernmental Panel on Climate Change*, 2000.

[33] Borken-Kleefeld, J., et al., *QUANTIFY transport emission scenarios up to 2100*, Environmental Science and Technology, 2010.